Appl. Phys. B 83, 219–223 (2006)
DOI: 10.1007/s00340-006-2157-6

Applied Physics B
Lasers and Optics

T. PALCHAN[1,✉]
S. EISENMANN[1]
A. ZIGLER[1]
D. KAGANOVICH[2]
R.F. HUBBARD[3]
M. FRAENKEL[4]
D. FISHER[4]
Z. HENIS[4]

All optical electron injector using an intense ultrashort pulse laser and a solid wire target

[1] Racah Institute of Physics, Hebrew University, Jerusalem, Israel
[2] LET Corp., Washington, DC 20007, USA
[3] Plasma Physics Division, Naval Research Laboratory, Washington, DC 20375, USA
[4] Plasma Physics Department, Soreq NRC, Yavne 81800, Israel

Received: 18 September 2005/
Revised version: 24 January 2006
Published online: 21 March 2006 •

ABSTRACT Energetic electron bunches were generated by irradiating a solid tungsten wire 13 μm wide with 50 femtosecond pulses at an intensity of $\sim 3 \times 10^{18}$ W/cm^2. The electron yield, energy spectrum and angular distribution were measured. These energetic electron bunches are suitable for injection into a laser driven plasma accelerator. An all-optical electron injector based on this approach could simplify timing and alignment in future laser-plasma accelerator experiments.

PACS 41.75.Ht; 41.75.Lx; 52.38.Kd; 52.38.Ph

1 Introduction

Present-day tabletop high power lasers based on the technique of chirped pulse amplification (CPA) [1] produce multiterawatt femtosecond laser pulses that can be used to drive plasma-based electron accelerators. In the laser wakefield accelerator (LWFA) [2–4, 6–19], the laser pulse excites a large amplitude plasma wave that propagates at nearly the speed of light and accelerates electrons to high energies over very short distances. However, LWFA acceleration experiments have primarily operated in the self-modulated (SM) regime, which relies on laser-plasma instabilities to produce the accelerating wakefield and generally produces poor quality electron beams with a large energy spread [11–19]. In the SM-LWFA, electrons are accelerated from the laser-produced plasma, so external electron injection is not required. The SM-LWFA operates in a high plasma density regime where the laser pulse length $c\tau_L$ is much shorter than the plasma wavelength $\lambda_p = 2\pi c\omega_p$, and ω_p is the electron plasma frequency. Recently, the breakthrough *bubble acceleration* approach that was proposed by Pukhov and Meyer-ter-Vehn several years ago, was verified experimentally [16–19]. Its unique feature is the generation of monochromatic electrons with energies up to 400 MeV [20]. However, significant pulse to pulse variations were observed.

It has been recognized for some time that the standard or resonant LWFA regime [2–4, 6–10], in which the laser pulse length is comparable to the plasma wavelength, offers a more promising path to producing a high quality electron beam. However, since accelerating gradients are generally smaller than in the SM-LWFA regime, the standard LWFA regime is expected to require external injection of electrons with sufficiently high axial velocity so that they can be trapped by the plasma wakefield before slipping behind the laser pulse. With phased external injection and optical guiding, available short pulse lasers are theoretically capable of producing high quality, stable GeV electron beams [6–8]. Although external injection could in principle be provided by a linac or RF gun, as has been done in an unguided standard LWFA experiment [9, 10], such systems are relatively large, and precise timing and alignment is difficult. There has also been considerable interest in all-optical injectors. Several optical injector concepts have been proposed, including LILAC (Laser Injected Laser Accelerator) [22], CP (colliding pulse) [23], and LIPA (Laser Ionization and Ponderomotive Acceleration) [24]. All of these concepts are theoretically capable of producing extremely short ($\ll 100$ fs), precisely-timed electron bunches with good beam quality, and all have been demonstrated experimentally to some extent. An SM-LWFA is also a potential all-optical injector candidate [11–19], although the beam produced is less suitable. However, optical injection into a separate LWFA acceleration stage presents substantial experimental challenges and has not yet been demonstrated.

In this work we describe a new optical injector concept that employs a femtosecond ultrahigh intensity laser pulse focused onto a metallic wire. This interaction produces a forward-directed beam of electrons with an energy spread of up to a few MeV. Strong phase bunching and good accelerated beam quality was shown by extensive simulations [25] using phased injection of test particles with a similar broad energy spectrum. With a proper choice of laser, plasma channel, and injected beam parameters, the LWFA can trap a significant fraction of the injected pulse while producing an ultrashort, high-quality accelerated pulse [26]. Energetic electrons from the interaction of ultrashort laser pulses with solid targets have been produced at a number of laboratories [24, 27–29]. However, most of these experiments have used foil targets, which presents geometrical difficulties for a LWFA application because the foil would block the accelerating laser pulse from the plasma acceleration region. The solid wire can be placed at a short distance from a plasma channel where the

✉ Fax: +972-2-6512483, E-mail: talap@phys.huji.ac.il

injected electrons can be further accelerated by a laser pulse. The plasma channel is used to guide the laser pulse at a high intensity, thereby increasing the interaction or acceleration length. Suitable plasma channels for guiding can be formed using capillary discharges [30], or line focused lasers with gas jets [32]. Since the wire can be placed very close to the plasma channel, this approach should be simpler to implement than other all-optical injection schemes. Although it may be possible to produce both the injected electrons and the channel-guided acceleration with a single laser pulse, it may be necessary to split the laser pulse in order to produce electrons at the proper phase for subsequent acceleration.

The energetic electrons were produced by focusing a linearly-polarized 6 TW laser onto a 13 μm diameter tungsten wire. The wire diameter chosen was smaller than the focused laser spot to allow a possibility of using a single laser beam for injection and acceleration. The proper phase match can be obtained by varying the distance between the wire and the capillary. The electrons were characterized both in their energy spectrum and angular distribution. The number and temperature of the electrons generated in this experiment differed significantly when the laser polarization was changed between S and P polarization, where P polarization means that the $\boldsymbol{E}$ vector of the laser field is parallel to the wire axis and the S polarization $\boldsymbol{E}$ vector perpendicular to the wire axis.

Section 2 describes the experimental setup. Section 3 presents measurements of electron energy spectra and angular distribution for both S and P polarization. Section 4 compares the measured energy spectra with the Boltzmann distribution expected for ponderomotive acceleration and discusses the polarization dependence. Section 5 describes transport of the injected electrons through a capillary discharge and discusses the role of fringing magnetic fields due to the current in the discharge. Results are summarized in Sect. 6.

2 Experimental setup

The experiments were conducted using a 6 TW short pulse Ti-sapphire laser with a wavelength of 800 nm. The laser delivered 45 fs FWHM pulses with a maximum energy up to 600 mJ at a pulse repetition rate of 10 Hz. A schematic drawing of the experimental set up is shown in Fig. 1. The laser beam was focused to a 30 μm diameter spot using an f/6 off-axis parabolic mirror at perpendicular incidence with respect to the target. The maximum intensity in the focal plane was estimated to be about 3×10^{18} W/cm^2. The contrast ratio of the main pulse to the prepulse that precedes it by 8 ns was greater than 10^4. The targets were solid tungsten wires 13 μm wide. For the purpose of comparison, electron generation from solid 25 μm thick tungsten foils was investigated as well.

The electron energy distribution in the forward direction was measured with a magnetic spectrometer. The detector was a BC-400 scintillator located at 19 cm from the backside surface of the target. The scintillator was 14 cm long and 2.5 mm thick and was coupled to an ICCD (Intensified Charged Coupled Device) Andor camera. A cylindrical collimator with an entrance opening of 3 mm was placed between the target and the scintillator. The collimator was made of 50 mm thick graphite and 5 mm lead. The scintillator was covered with two layers of 20 μm Al foil as a light shield that prevented light penetration without affecting electrons with energies above 100 keV. For electrons in the energy range between 100 keV and a few MeV, the number of photons created in this scintillator is proportional to the number of electrons, although there is a difference in penetration depth at different energies. This feature allowed us to obtain the number of electrons and to derive their energy distribution.

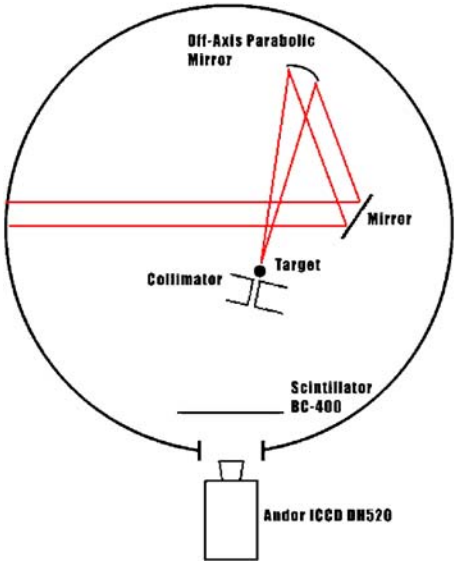

FIGURE 1 Experimental setup. The laser is focused by an off-axis parabola onto a wire target, producing energetic electrons. These electrons pass through a collimator and are deflected by a vertical magnetic field and detected by the scintillator

Energetic electron spectra were measured for both P and S laser polarization. The angular distribution of the electrons was also measured using a curved film that was placed at 5 cm from the target and surrounded the target over a 180° angle. A 30 μm thick Al filter was inserted in front of the film to block direct laser light and soft X-rays. Electrons with energies lower than ∼ 100 keV did not penetrate the filter.

3 Measurements of electron energy spectra

Figure 2 shows an example of the electron image recorded by the ICCD camera in an experiment with a ver-

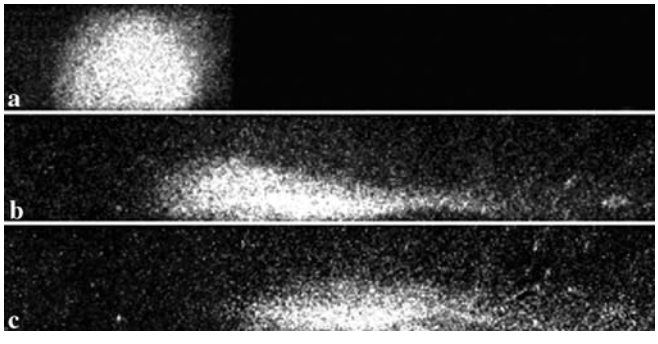

FIGURE 2 The electron image recorded by the ICCD camera in an experiment with a vertical wire target, P laser polarization and a magnetic field of 83 Gauss (**a**), 40 Gauss (**b**) and no magnetic field (**c**)

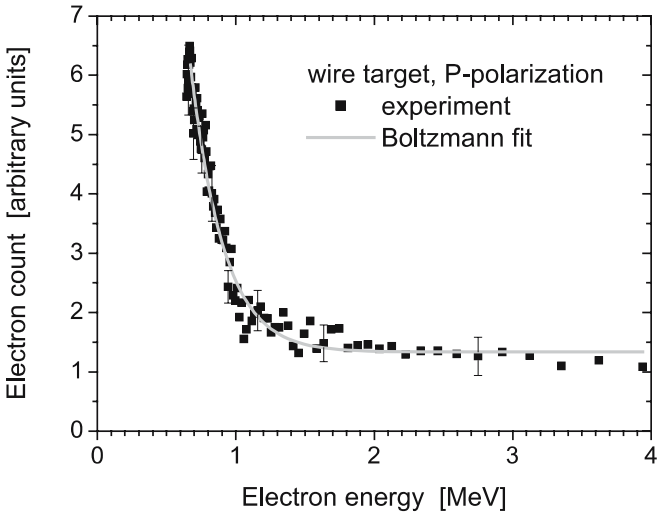

FIGURE 3 Spectrum of fast electrons measured in the forward laser direction for irradiation of a wire target with P laser polarization

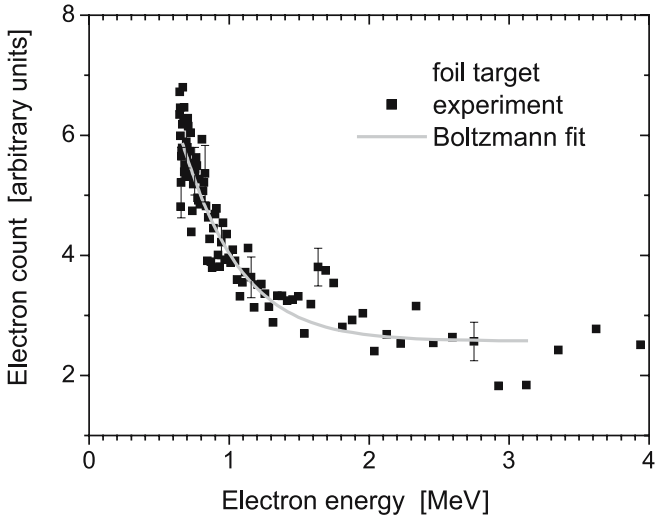

FIGURE 5 Spectrum of fast electrons measured in the forward laser direction for irradiation of 25 μm foil targets with P laser polarization

tical wire target and P laser polarization. The three images correspond to spectrometer magnetic fields of (a) 83 Gauss, (b) 40 Gauss, and (c) zero Gauss. The energy of the electrons was derived from the calculation of electron trajectories using a map of the measured magnetic field.

Figures 3 and 4 show the energy spectrum of electrons generated from wire targets for P and S polarization. The number of electrons calculated from the integrated spectrum was about 1.5×10^6 per pulse for wire targets under laser P polarization. The electron yield was about 20% less for S polarization. The electron density spectrum peaked at about 600–700 keV. A tail of hotter electrons with energies of up to 3 MeV is seen in the spectrum; however their number is close to the noise level of the detection system. The cutoff on the low energy part of the spectrum can be attributed to the strong space charge field created on the surface of the wire. This field only allows escape of the energetic electrons. The peak of the electron distribution can be controlled by the laser intensity and can be tuned for optimal conditions of electron injection. The curves in Figs. 3 and 4 are Boltzmann fits to the experimental data.

Figure 5 shows the energy spectrum of electrons generated from 25 μm thick foil targets for P laser polarization. In this case, the electron generation is not enhanced for laser P polarization, as measured for the case of a wire target.

The angular distribution of energetic electrons was measured by removing the collimator and surrounding the target in the forward direction with AGFA D-7 film. The film was bent into a semicircular shape and placed 5 cm from the target, thus providing angular coverage of 180°. This film is relatively insensitive to energetic X-rays and highly sensitive to charged particles. The influence of relatively low energy X-rays and electrons with energy below 100 keV was eliminated by using a 200 μm Al foil in front of the film. The angular distribution of forward electrons and the raw film image are shown in Fig. 6. The angular distribution of the electrons emitted in the

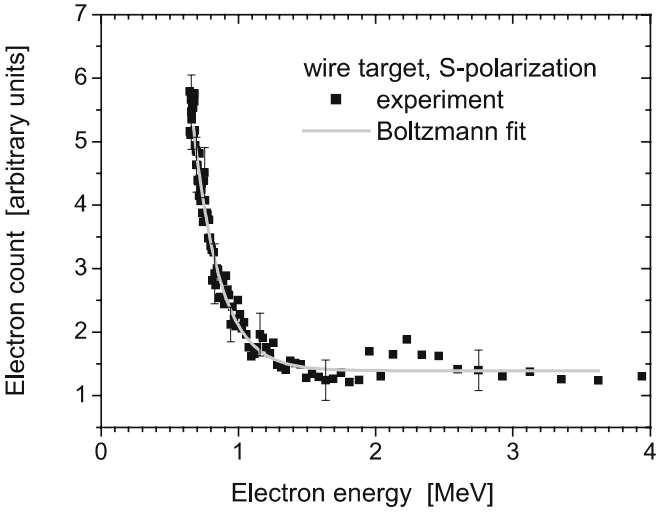

FIGURE 4 Spectrum of fast electrons measured in the forward laser direction for irradiation of a wire target with S laser polarization

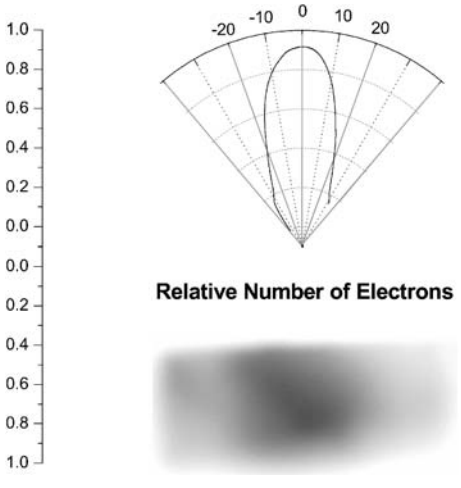

FIGURE 6 The angular distribution relative to the laser forward direction of the energetic electrons emitted from a wire target. The raw film image is shown at the *bottom* of the figure

forward direction shows a beam of collimated electrons moving within $\sim 20^\circ$ of the direction of laser propagation. This narrow bunch is accompanied by a low intensity ring with an angular spread of $\sim 50^\circ$.

4 Interpretation of electron energy spectra

The energy spectrum of hot electrons generated by ultrashort laser pulses is usually well described by a Boltzmann distribution with an effective temperature T_h. For electrons generated by ponderomotive acceleration [29, 32, 33], and laser intensity between 10^{18} and 10^{19} W/cm^2, this temperature is related to the ponderomotive potential by [27]

$$k_B T_h = m_0 c^2 \left(\sqrt{1 + I\lambda^2[\mathrm{W/cm^2\,\mu m^2}]/1.38 \cdot 10^{18}} - 1\right). \quad (1)$$

For $I = 3 \times 10^{18}$ W/cm^2, and $\lambda = 0.8$ μm, the predicted temperature is 273 keV. The electron temperatures were estimated by fitting experimental spectral data to a Boltzmann distribution

$$f(E) = \frac{\mathrm{d}N}{\mathrm{d}E} \sim \frac{E^{1/2}}{T_h^{3/2}} \exp\left(-\frac{E}{kT_h}\right), \quad (2)$$

in the range between 500 keV and 1 MeV. Figure 7 compares the results of the Boltzmann fits of the spectra in Figs. 3–5 to the ponderomotive scaling, $T_h = 273$ keV. The fitted electron temperature for the foil target experiments (329 keV) agrees well with the ponderomotive value. For wire targets, the fitted electron temperature is substantially lower.

The lower temperature obtained for the wire targets may be due to difficulties in focusing the laser beam onto these targets. Another explanation for this lower electron temperature may be related to the geometry of the wire experiment. If the fast electrons are produced by ponderomotive acceleration in the plasma generated on the surface of the solid target, the electron energy gain should be larger for cases with a larger plasma scale length. The plasma scale length on the wire surface is probably significantly smaller than that for the foil, due to two-dimensional geometrical effects and the fact that the wire is a factor of two thinner than the foil.

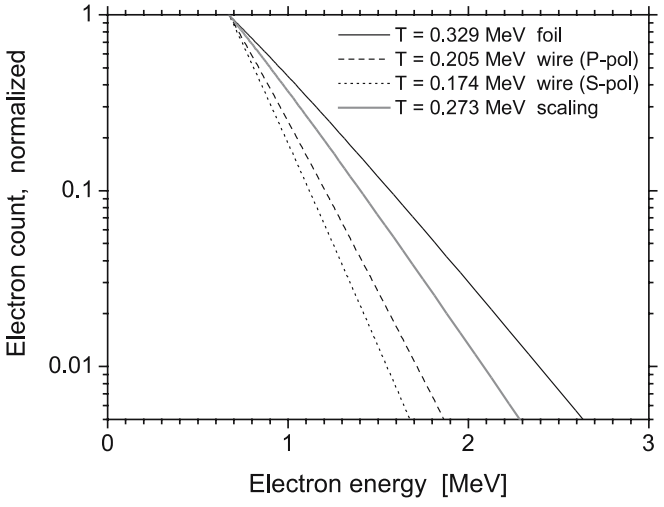

FIGURE 7 Normalized Boltzmann fit to the energy spectra of the electrons emitted from wire targets for P and S laser polarization, foil target. The fourth curve ($T = 0.273$ MeV) gives the theoretical ponderomotive scaling based on (1)

The data obtained from wire targets also exhibits polarization dependence. The fitted temperatures are 205 keV for laser P polarization and 174 keV for S polarization in the case of wire targets. These polarization differences may be related to the appearance of additional mechanisms such as resonance absorption [32–34]. For wire targets with width smaller than the diameter of the laser spot, the laser electric field has a non-zero component perpendicular to the target at normal incidence, and resonance absorption may occur during the irradiation. This process may contribute to the increase in the number of electrons in the case of a P polarized laser beam. Alternatively, a mechanism known as Brunel (or vacuum) heating [35] may be more efficient for energetic electron generation in the case of P polarization. In Brunel heating the electrons are pulled into vacuum in one half-cycle of the laser field, accelerated in vacuum, and re-injected into the dense region and farther into the target in the next half-cycle. In the case of a wire target, it may be possible that electrons that are pulled from the sides of the wire will subsequently be accelerated away from the target.

5 Transport of electrons through a capillary discharge

In order for a capillary discharge to be suitable for a channel-guided LWFA, energetic electrons must be injected into the capillary with high efficiency and transported without substantial losses. The electrical current in the discharge produces substantial magnetic fields that can affect electron trajectories both inside and outside the capillary. For the LWFA parameter regime, the electromagnetic fields produced by the laser plasma interaction are generally much larger than the discharge fields. However, the fringing magnetic fields in the region just outside the discharge could deflect the externally-injected electrons and cause them to be lost. This problem was recently examined theoretically by Hafizi et al. [36], who concluded that for typical LWFA parameters, the deflection of injected electrons by the magnetic field of the discharge should be small compared with the acceptance of the wakefield.

A series of shots was taken in which electrons from a wire target were injected into a capillary discharge. The polarity of the discharge current was chosen such that the magnetic field inside the capillary confined the electrons. The standoff distance between the wire and the entrance to the capillary was 500 μm. The average number of electrons transported through the capillary was 1.49×10^6 when the capillary current was triggered. When no discharge current was triggered, the capillary acted as a simple collimator, and the average number of electrons transported was actually slightly lower (1.41×10^6). These results are consistent with the theoretical model [36] and suggest that there were no significant losses due to magnetic fields outside the capillary.

6 Conclusions

In conclusion, electron bunches with energies up to several MeV were generated by irradiating tungsten wires with 45 fs, 3×10^{18} W/cm^2, 10 Hz laser pulses. The energetic

electron yield was about 1.5×10^6 per pulse into a 20° cone. This energetic electron bunch will be used as an optical injector for a channel-guided laser wakefield accelerator. The proposed method provides the possibility of simplified timing between injection and acceleration.

ACKNOWLEDGEMENTS The authors acknowledge useful discussions with G. Marcus, Y. Horowitz, S. Elieser, B. Hafizi, and D.F. Gordon. Several authors (DK, RFH) acknowledge support from the Department of Energy and the Office of Naval Research.

REFERENCES

1 D. Strickland, G. Mourou, Opt. Commun. **56**, 219 (1985)
2 T. Tajima, J.M. Dawson, Phys. Rev. Lett. **43**, 267 (1979)
3 E. Esarey, P. Sprangle, J. Krall, A. Ting, IEEE Trans. Plasma Sci. **24**, 252 (1996) and references therein
4 P. Sprangle, E. Esarey, A. Ting, G. Joyce, Appl. Phys. Lett. **53**, 2146 (1988)
5 L.M. Gorbunov, V.I. Kirsanov, Sov. Phys. JETP **66**, 290 (1987)
6 R.F. Hubbard, D. Kaganovich, B. Hafizi, C.I. Moore, P. Sprangle, A. Ting, A. Zigler, Phys. Rev. E **63**, 036 502 (2001)
7 P. Sprangle, B. Hafizi, J.R. Peñano, R.F. Hubbard, A. Ting, C.I. Moore, D.F. Gordon, A. Zigler, D. Kaganovich, T.M. Antonsen, Phys. Rev. E **63**, 056 405 (2001)
8 W.P. Leemans, C.W. Siders, E. Esarey, N.E. Andreev, G. Shvets, W.B. Mori, IEEE Trans. Plasma Sci. **24**, 331 (1996)
9 F. Amiranoff, S. Baton, D. Bernard, B. Cros, D. Descamps, F. Dorchies, F. Jacquet, V. Malka, J.R. Marquès, G. Matthieussent, P. Miné, A. Modena, P. Mora, J. Morillo, Z. Najmudin, Phys. Rev. Lett. **81**, 995 (1998)
10 F. Dorchies, F. Amiranoff, V. Malka, J.R. Marques, A. Modena, D. Bernard, F. Jacquet, P. Mine, B. Cros, G. Matthieussent, P. Mora, A. Solodov, J. Morillo, Z. Najmudin, Phys. Plasmas **6**, 2903 (1999)
11 A. Modena, Z. Najmudin, A.E. Dangor, C.E. Clayton, K.A. Marsh, C. Joshi, V. Malka, C.B. Darrow, C. Danson, IEEE Trans. Plasma Sci. **PS-24**, 289 (1996)
12 D. Gordon, K.C. Tzeng, C.E. Clayton, A.E. Dangor, V. Malka, K.A. Marsh, A. Modena, W.B. Mori, P. Muggli, Z. Najmudin, D. Neely, C. Danson, C. Joshi, Phys. Rev. Lett. **82**, 2133 (1998)
13 C. Gahn, G.D. Tsakiris, G. Pretzler, K.J. Witte, P. Thirolf, D. Habs, C. Delfin, C.G. Wahlström, Phys. Plasmas **9**, 987 (2002)
14 C.I. Moore, A. Ting, K. Krushelnick, E. Esarey, R.F. Hubbard, B. Hafizi, H.R. Burris, C. Manka, P. Sprangle, Phys. Rev. Lett. **79**, 3909 (1997)
15 V. Malka, J. Faure, J.R. Marque, F. Amiranoff, J.P. Rousseau, S. Ranc, J.P. Chamberet, Z. Najmudin, B. Walton, P. Mora, A. Solodov, Phys. Plasmas **8**, 2605 (2001)
16 S.P.D. Mangles, C.D. Murphy, Z. Najmudin, A.G.R. Thomas, J.L. Collier, A.E. Dangor, E.J. Divall, P.S. Foster, J.G. Gallacher, C.J. Hooker, D.A. Jaroszynski, A.J. Langley, W.B. Mori, P.A. Norreys, F.S. Tsung, R. Viskup, B.R. Walton, K. Krushelnick, Nature **431**, 535 (2004)
17 C.G.R. Geddes, C. Toth, J. van Tilborg, E. Esarey, C.B. Schroeder, D. Bruhwiler, C. Nieter, J. Cary, W.P. Leemans, Nature **431**, 538 (2004)
18 J. Faure, Y. Glinec, A. Pukhov, S. Kiselev, S. Gordienko, E. Lefebvre, J.P. Rousseau, F. Burgy, V. Malka, Nature **431**, 541 (2004)
19 A. Pukhov, J. Meyer-ter-Vehn, Appl. Phys. B **74**, 355 (2002)
20 V. Malka et al., ICF Workshop on Laser-Beam Interaction and Plasma Accelerators, National Taiwan University, Taipei, Taiwan, Dec (2005)
21 D. Giulietti, M. Galimberti, A. Giulietti, L.A. Gizzi, M. Borghesi, P. Balcou, A. Rousse, J.P. Rousseau, Phys. Rev E **64**, 015 402 (2001)
22 D. Umstadter, J.K. Kim, E. Dodd, Phys. Rev. Lett. **76**, 2073 (1966)
23 E. Esarey, R.F. Hubbard, W.P. Leemans, A. Ting, P. Sprangle, Phys. Rev. Lett. **79**, 2682 (1997)
24 C.I. Moore, A. Ting, S.J. McNaught, J. Qiu, H.E. Burris, P. Sprangle, Phys. Rev. Lett. **82**, 1688 (1999)
25 R.F. Hubbard, D.F. Gordon, T. Jones, J.R. Peñano, P. Sprangle, A. Ting, B. Hafizi, A. Zigler, D. Kaganovich, in *Proc. 2003 Particle Accelerator Conf.*, Inst. of Electrical and Electronic Eng., Piscataway, NJ (2003) p. 716
26 D. Gordon, J.H. Cooley, P. Sprangle, B. Hafizi, R.F. Hubbard, Phys. Rev. E **71**, 026 404 (2005)
27 P.V. Nickles, M.P. Kalachnikov, P.J. Warwick, K.A. Janulewicz, W. Sadner, U. Jahnke, D. Hilscher, M. Schnürer, R. Nolte, A. Rousse, Quantum Electron **QE-29**, 444 (1999)
28 K. Nakajima, D. Fisher, T. Kawakubo, H. Hashaniki, A. Ogata, Y. Kato, Y. Kitagawa, R. Kodama, K. Mima, H. Shiraga, K. Suzuki, K. Yamakawa, T. Zhang, Y. Sakawa, T. Shoji, Y. Nishida, N. Yagami, M. Downer, T. Tajima, Phys. Rev. Lett. **74**, 4428 (1995)
29 G. Malka, J.L. Miquel, Phys. Rev. Lett. **77**, 75 (1996)
30 Y. Ehrlich, A. Zigler, C. Cohen, J. Krall, P. Sprangle, Phys. Rev. Lett. **77**, 4186 (1996)
31 C.G. Durfee, H.M. Milchberg, Phys. Rev. E **71**, 2409 (1993)
32 S.C. Wilks, W.L. Kruer, M. Tabak, A.B. Langdon, Phys. Rev. Lett. **69**, 1383 (1992)
33 S.C. Wilks, W.L. Kruer, IEEE J. Quantum Electron. **QE-33**, 1954 (1997)
34 N.H. Ebrahim, H.A. Baldis, C. Joshi, R. Benech, Phys. Rev. Lett. **45**, 1179 (1980)
35 F. Brunel, Phys. Rev. Lett. **59**, 52 (1987)
36 B. Hafizi, D.F. Gordon, A. Zigler, A. Ting, Phys. Plasmas **10**, 2545 (2003)